AIIM

Association for Information and Image Management

1100 Wayne Avenue, Suite 1100
Silver Spring, Maryland 20910

301/587-8202

Centimeter

Inches

MANUFACTURED TO AIIM STANDARDS
BY APPLIED IMAGE, INC.

1 of 1

BNL-60611

SEISMIC SAFETY OF EARTH DAMS. A PROBABILISTIC APPROACH

N. Simos, C.J. Costantino and M. Reich
Department of Advanced Technology
Brookhaven National Laboratory, Upton, NY 11973

ABSTRACT

The evaluation of the potential for slope sliding and/or liquefaction failure of earthen dams subjected to earthquake loadings is most often based on deterministic procedures of both the excitation input and of the physical model. Such treatment provides answers in the form of either factor of safety values or a yes or no as to whether liquefaction will occur or not. Uncertainties in the physical properties of the soil in the embankment and the foundation layers underlying the dam are typically treated with parametric studies. While extensive soil testing can compensate for the luck of such information, questions on what deterministic earthquake to use as representative of the site remain.

Consideration of probabilities pertaining to the uncertainties of the earthquake and of the site characterization is expected to augment the prediction of failure potential by associating slope and liquefaction failure to generic properties of the earthquake and of the site characterization. In this study, the procedures for conditional slope failure/liquefaction probabilities are formulated based on a series of simulated deterministic analyses of a dam cross section. These synthetic earthquakes emanate from a 1-D stationary stochastic process of zero mean and an analytical form of power spectral density function.

The response of the dam section is formed upon a dynamic finite element approach which provides the temporal variations of the stresses, strains and pore water pressure throughout the model. The constitutive response of the granular soil skeleton and its coupling with the fluid phase is formulated based on the Biot dynamic equations of motion with nonlinear terms compensated for into soil hysteretic damping. Lastly, a stochastic approach to liquefaction based on the transfering of the input motion statistics to the cross section is presented.

1.0 Introduction

During an earthquake event of considerable duration and intensity an earthen dam can experience partial or total failure that stems from either loss of soil strength due to liquefaction or reduction of the inherent resistance to sliding along a potential failure surface. In trying to assess the potential to failure in either mode one has to essentially incorporate two types of probabilities. One that is associated with the occurance of an earthquake in the proximity of the structure and the other with the state of the soil and its tendency to liquefy or fail in shear.

The coupling of the two essential components (excitation and soil state) with inherent statistical properties can only be achieved through response analyses that allow for the combined statistics to participate. A promising approach is the one involving the Unit Response of the domain that can eventually provide the system response resulting from a seismic event which in turn represents a stochastic process. Such procedure, however, implies that the domain exhibits linear behavior. While in typical soils this is only true in small strains, the benefits of the Unit Response approach compensate for the lack of nonlinear considerations.

For a study case a hypothetical earth dam built over a saturated soil layer was considered, Figure 1. The constitutive response of the granular soil skeleton and its coupling with the fluid phase is formulated around the Biot dynamic equations of motion. The finite element analysis utilized in the evaluation of the dynamic response is a linear in character but it treats the soil as a two-phase medium. While the drawback of linearity is somewhat compensated with the equivalent hysteretic damping,

This work was done under the auspices of the U.S. Dept. of Energy.

it is the two-dimensional pore water/soil sceleton interaction that provides a realistic description of the behavior of the soil in a dynamic mode. The solution takes place in the frequency domain and the resulting harmonic response, inverted with the use of Fast Fourier Transform techniques, provides the intergranular stress as well as the pore water pressure fluctuation during the seismic event.

The failure potential, viewed in the form of a factor of safety against slope failure, is evaluated by incorporating the *in-situ* and seismically induced dynamic stresses over various potential surfaces were sliding can occur during an earthquake event. The driving forces in the liquefaction process is the dynamic (cyclic) shear stress that is generated in the soil layers and the buildup of pore pressures. While a linear analysis cannot predict the buildup and the dissipation of the pore pressures, it can provide the level of shearing that the soil experiences during the seismic event. This in turn can become the basis for assessing the susceptibility to liquefaction

2.0 Seismic Response of a Dam

Initial Effective Stress State

The stress field prior to a seismic event that exists in the embankment and the foundation layer are an important element in the stability integrity evaluation. The static stress conditions are key components in the definition of the factor of safety against slope failure. Further, the overburden initial stress is vital to a liquefaction potential analysis because of its relation with the effective stress that controls the process of liquefaction.

For the case of a saturated medium, the initial total stress vector

$$[\tau^0] = [\tau^0_{xx} \quad \tau^0_{yy} \quad \tau^0_{xy}]^T$$

is computed by POROSLAM. These stresses are the result of the body forces while taking into account the presence of water in the pores (increased effective density) and the hydrostatic loads resulting from the reservoir behind the dam.

The stress field in the system is the result of the soil overburden and of the hydrostatic action of the water in the reservoir. The discretized cross section of the embankment and its foundation are considered to be in a plane strain state of stress while values of the elastic properties for the different soils were assumed.

The effective overburden stress σ_0 is deduced from the relation,

$$\sigma_0 = \tau^0_{yy} - \alpha p_f \qquad (1)$$

where τ_{yy} is the overburden stress, α is the compressibility of the soil fraction and p_f is the pore pressure deduced from the solution of the equation governing seepage

$$k_x \frac{\vartheta h(x,y)}{\vartheta x^2} + k_y \frac{\vartheta h(x,y)}{\vartheta y^2} = 0 \qquad (2)$$

and the relation

$$p_f = h - y \qquad (3)$$

where, $h(x,y)$ = total head and k_x, k_y = soil permeabilities.

Dynamic analysis of the 2-phase medium

In assessing the dynamic response of the embankment-foundation the saturated state of the soil must be accounted for. The pore pressure of the water trapped in the soil skeleton will fluctuate during the earthquake and impact on the intergranular soil stresses. Since the strength of the soil is tied to the intergranular stresses, it is vital that the dynamic pore pressure be captured. The coupled behavior of pore water and soil skeleton requires that the medium must be treated as a two-phase one with governing equations that reflect the coupling.

Further, the ability of the soil to resist liquefaction is one hand dependent on its initial stress state (effective stress) and on the other on the intensity of the dynamic shear stress. The shear stress variation at different locations in the embankment and the foundation as well as the number of stress cycles during the earthquake event determine whether the soil is susceptible to such failure.

Therefore, to effectively analyze the system, the employed theoretical/computational model must enable;

a. The description of the domain as a two-phase medium.
b. The implementation of actual or representative earthquake input.
c. The evaluation of the time variation of stresses resulting from the seismic input.

In order to perform the dynamic analysis, which satisfies the above requirements, the POROSLAM code is employed. The code is a two-dimensional finite element representation of Biot's dynamic equations for both soil and fluid phases. Biot's equations are a linear description of the response of the soil skeleton and of the pore water in the form,

$$\frac{\vartheta \tau_{xx}}{\vartheta x} + \frac{\vartheta \tau_{xy}}{\vartheta y} = \varrho \ddot{u}_x + \varrho_f \ddot{w}_x$$

$$\frac{\vartheta \tau_{yx}}{\vartheta x} + \frac{\vartheta \tau_{yy}}{\vartheta y} = \varrho \ddot{u}_y + \varrho_f \ddot{w}_y$$

and

$$-\frac{\vartheta p_f}{\vartheta x} = \varrho_f \ddot{u}_x + \frac{1}{f}\varrho_f \ddot{w}_x + \frac{\eta}{k}\dot{w}_x$$

$$-\frac{\vartheta p_f}{\vartheta y} = \varrho_f \ddot{u}_y + \frac{1}{f}\varrho_f \ddot{w}_y + \frac{\eta}{k}\dot{w}_y \quad (4)$$

where,

$[u_x, u_y]$ = components of displacement of the soil

$[w_x, w_y]$ = components of displacement of the pore water

$$\{\tau\} = (\tau_{xx}, \tau_{yy}, \tau_{xy})^T =$$

$$\{\sigma_{xx} - \alpha p_f, \sigma_{yy} - \alpha p_f, \sigma_{xy}\}^T$$

while, f = porosity, ϱ = total mass density, ϱ_f = fluid mass density, α = compressibility of solid, M = compressibilityof the fluid, η = fluid viscosity and k = soil permeability.

The resultant equation that expresses the total stress vector in terms of the displacement vector while considering hysteretic damping, takes the form

$$\{\tau\} = E_c [D_1] \left([D_0] + [D_3] \frac{\vartheta}{\vartheta t} \right) \{u_x, u_y\}^T +$$

$$\alpha^2 M [D_2] \{u_x, u_y\}^T + \alpha M [D_2] \{w_x, w_y\}^T \quad (5)$$

where,

$$[D_0] = \begin{bmatrix} 1 & \frac{\nu}{1-\nu} & 0 \\ \frac{\nu}{1-\nu} & 1 & 0 \\ 0 & 0 & \frac{1-2\nu}{2(1-\nu)} \end{bmatrix}$$

$$[D_3] = \begin{bmatrix} \lambda_c & \frac{\lambda_c \nu}{1-\nu} & 0 \\ \frac{\lambda_c \nu}{1-\nu} & \lambda_c & 0 \\ 0 & 0 & \frac{\lambda_s (1-2\nu)}{2(1-\nu)} \end{bmatrix}$$

$$[D_1] = \begin{bmatrix} \frac{\vartheta}{\vartheta x} & 0 \\ 0 & \frac{\vartheta}{\vartheta y} \\ \frac{\vartheta}{\vartheta y} & \frac{\vartheta}{\vartheta x} \end{bmatrix} \qquad [D_2] = \begin{bmatrix} \frac{\vartheta}{\vartheta x} & \frac{\vartheta}{\vartheta y} \\ \frac{\vartheta}{\vartheta x} & \frac{\vartheta}{\vartheta y} \\ 0 & 0 \end{bmatrix}$$

$$p_f = -\alpha M (e_{xx} + e_{yy}) - M \left(\frac{\vartheta w_x}{\vartheta x} + \frac{\vartheta w_y}{\vartheta y} \right)$$

λ_c is the hysteretic damping ratio associated with hydrostatic compression while λ_s represents the damping ratio associated with shear strains and $E_c = \frac{(1-\nu)E}{(1+\nu)(1-2\nu)}$.

The implementation of transmiting boundaries on the two sides of the model allow for the propagation of waves outward. These boundaries ensure the continuation of both intergranular stresses and pore pressures in the saturated soil. The propagation is based on the one-dimensional wave equations of saturated soils where,

$$\tau_{xx} = E_c \left(\frac{\vartheta u_x}{\vartheta x} + \lambda_c \frac{\vartheta}{\vartheta t} \frac{\vartheta u_x}{\vartheta x} \right)$$

$$+\alpha^2 M \frac{\vartheta u_x}{\vartheta x} + \alpha M \frac{\vartheta w_x}{\vartheta x}$$

$$p_f = -\alpha M \frac{\vartheta u_x}{\vartheta x} - M \frac{\vartheta w_x}{\vartheta x} \quad (6)$$

while shear transmission is governed by the principle :

$$\tau_{xy} = \varrho V_s \dot{u}_s \qquad (7)$$

where $\dot{u}_s$ = velocity in the direction of shear and V_s = shear wave velocity of the soil.

Harmonic Solution

The dynamic input can be either **deterministic** or **stochastic**. In the deterministic mode the given ground excitations or dynamic loads are expressed in the following form

$$g(t) = \sum_{k=1}^{N} X(\omega)\, e^{i\omega_k t}$$

where ω_k are the frequencies of the harmonic analysis. In the stochastic mode the base excitation or the forcing function is expressed in terms of the complex input

$$X(\omega_k) = e^{i\omega_k t}$$

Evaluation of the response at the frequencies ω_k leads to the complex frequency response $H(\omega)$. The Fourier coefficients of a response quantity $Y(\omega)$ (displacement or stress) from a synthetic input with coefficients $X(\omega)$ can be obtained through the relation

$$Y(\omega) = H(\omega)\, X(\omega) \qquad (8)$$

In probabilistic analysis that is based on a Monte Carlo scheme (multiple evaluation of the response at the same intensity level but with random distribution of peaks) the simulated earthquakes or dynamic loads belong to a certain family. Such family can be characterized by a **response** or a **power spectrum**. Earthquake (or load) records can be synthesized on the basis of these properties. For the case of an earthquake family described by the **Kanai-Tajimi** power spectrum

$$S_x(\omega, \lambda) = S_0 \frac{1 + 4\zeta_g^2 \left(\frac{\omega}{\omega_g}\right)^2}{\left[1 - \left(\frac{\omega}{\omega_g}\right)^2\right]^2 + 4\zeta_g^2 \left(\frac{\omega}{\omega_g}\right)^2}$$

$$\lambda = \left[\zeta_g, \omega_g, S_0\right]^T \qquad (9)$$

the synthetic time history $g(t)$ generated from the form

$$g(t) = 2\zeta(t) \sum_{i=1}^{N} \sqrt{S_x(\omega_i)\, \Delta\omega} \cos(\omega_i t + \phi_i) \qquad (10)$$

is a realization of the process described by the power spectrum. In order to accommodate the non-stationary part of the ground excitation, the simulated acceleration or force is multiplied by the nonstationary function $\zeta(t)$. In the above expression

$$w_i = i\Delta\omega \qquad \Delta\omega = \frac{\omega_u}{N}$$

where ω_u is a cutoff frequency and ϕ_i is a vector of random phase angles uniformly distributed between 0 and 2π. Different choices of the vector of random phase angles will lead to a different simulated dynamic inputs. The synthetic process $g(t)$ is periodic with a period $T_0 = \frac{2\pi}{\Delta\omega}$.

3.0 Evaluation of Failure Potentials

Slope Failure

The stability of the dam is viewed in terms of a safety factor along any potential failure surface as shown in Figure 1. The margin of safety against slope sliding can typically be seen as the ratio of the shear strength at a given effective stress to the corresponding shear strength on the envelope line. While debate surrounds the definition of an appropriate safety factor, in this analysis safety factor is defined in terms of the state of stress at any instant during the seismic event through the stress invariants of the intergranular stresses.

Since failure is expected to occur over an entire plane, the safety factor along any such potential surface is defined as a contribution from all the points transversed by the surface as follows,

$$SF = \frac{\sum_i A_i SF_i}{\sum_i A_i} \qquad (11)$$

where A_i = area of the finite element transversed by failure surface and $(SF)_i$ = safety factor for element i. The safety factor for an individual element is formed on the basis of the intergranular stress invariants J_1 and J_2' and the Mohr-Coulomb failure envelope where,

$$-\alpha J_1 + \sqrt{J_2'} = k$$

$$J_1 = \sigma_x + \sigma_y + \sigma_z$$

$$J_2' = \frac{\left[(\sigma_x - \sigma_y)^2 + (\sigma_y - \sigma_z)^2 + (\sigma_z - \sigma_x)^2\right]}{6} + \tau_{xy}^2 \qquad (12)$$

$$k = \frac{3C}{\sqrt{9 + 12tan^2\phi}} \qquad \alpha = \frac{tan\phi}{\sqrt{9 + 12tan^2\phi}}$$

such that

$$SF_i = \frac{k + \alpha J_1}{\sqrt{J_2'}} \qquad (13)$$

Three parameters are expected to greatly influence the safety factor defined above, namely the intensity of the ground acceleration as well as its spectral characteristics, the frictional angle ϕ and the hysteretic damping of the soil.

Because of the linearity of the constitutive equations, the dynamic stresses that will result from a scaled-up earthquake will be subject to similar increase, except for the effects of the hysteresis. The amplification of the fluctuation of the intergranular stresses and pore pressures will, at various times of the seismic duration, bring the stress state of the points closer to the failure surface causing significant reduction of the safety factor. This issue is addressed with the evaluation of the safety factor over a chosen failure surface subject to incremental changes of the peak acceleration of the same earthquake. Figure 2 depicts (a) a typical acceleration record acting as base excitation to the dam section, (b) the temporal variation of the dynamic shear stress at a particular location induced by the input excitation and (c) the temporal variation of the safety factor along a selected failure surface.

Liquefaction potential

Two methods both built into the program can be utilized in assessing liquefaction susceptibility. The first has been introduced by Seed & Idriss and is called **Simplified Liquefaction Procedure**. It represents the classical method used in evaluating liquefaction susceptibility. The second approach is a **Probabilistic method** that reflects the statistics of the excitation and it estimates probability of failure. In applying either method the following observations must be considered. Liquefaction potential has been assessed to be greatly affected by certain parameters participating during the dynamic event. These include the soil type, the initial effective stress and the nature of the excitation (*i.e.* earthquake type). Consequently, the soil type with inherent damping and the intensity and type of the input determine the intensity and the cyclic profile of the dynamic shear stresses.

a. soil type

It has been observed that sand deposits are more susceptible to liquefaction than deposits of silt, clay, gravel or coarse sands. This is attributed to the uniform grading of the sand as compared to the other soil types. The susceptibility of the soil to liquefaction also depends on its void ratio or *relative density*. The looser the sand the higher the potential for liquefaction for a given earthquake.

b. initial effective stress

It has been observed in laboratory tests that there is a direct link between the stress required to initiate liquefaction under cyclic load and the effective stress at the location of interest. Specifically, the required driving stress (or soil strength) increases with increased effective stress.

c. dynamic input properties

The vulnerability of the soil to liquefaction is determined by the level of stress or strain that develops during a dynamic event. For a shear stress failure the developed stress in the soil must exceed the soil strength while for a strain driven failure the threshold strain must be exceeded. The shear

stresses or strains that develop in the soil are directly related to the intensity of the earthquake. In laboratory tests the soil, subjected to a cyclic load of a given intensity, fails after a number of such loading cycles. In the field and under the action of an earthquake, the event must have enough duration such that a significant number of loading cycles can develop. These cycles are not uniform, but they can effectively be represented by an equivalent uniform cycle record.

Simplified Liquefaction Procedure

This Seed & Idriss process is outlined in the following steps:

a. Definition of the earthquake that is likely to occur at/or in the vicinity of the site and application as base excitation. The excitation in the seismic liquefaction process is considered to be vertically propagating shear waves (shear stresses govern the process).

b. Calculation of the time history record of the intergrannular shear stresses at selected locations.

c. Transformation of the time history of the shear stress into an equivalent record of uniform intensity. This is based on strength data for the particular soil similar to the ones in Figure 3 and achieved with the relation

$$N_{eq} = \sum_{i=1}^{n} \frac{N_i}{N_i^{eq}} N_{av} \qquad (14)$$

where,

N_{eq} = Equivalent Uniform Cycles
N_i = Induced Shear stress cycles at level $\frac{\tau_i}{\sigma_0}$
N_i^{eq} = Equivalent uniform cycles causing liquefaction at τ_i
N_{av} = Stress cycles inducing liquefaction at $\tau_{av} = 0.65\tau_{max}$

d. Evaluation of the soil strength $(\frac{\tau}{\sigma_0})_{eq}$ from the equivalent uniform cycles.

e. Computation of the factor of safety against liquefaction according to the relation

$$LQF = \frac{Strength \quad at \quad N_{equiv}}{0.65 \quad \tau_{max}} \qquad (15)$$

for the shear mode. For complex stress state, however, where the impiging seismic waves are not only shear waves it is sugested that similar strength curves be developed (from laboratory tests) reflecting the strength of the soil as a function of more than just the shear stress. This can be achieved through the stress invariant $\sqrt{J_2}'$. The liquefaction safety factor can then be equivalently defined as

$$LQF = \frac{\sqrt{J'_2}_{soil \quad testing}}{\sqrt{J'_2}_{seismically \quad induced}}$$

For either approach the index LQF will determine the liquefaction susceptibility of the soil at the given location ($LQF > 1.0$: no liquefaction).

4.0 Stochastic Assessment of Failure

POROSLAM Probabilistic Analysis. Monte Carlo Simulations

The process built in the program can apply to assessments of either slope failure or liquefaction. For either option a **conditional limit state** is defined as

$$F_{SF} = (SF) - 1.0 = 0$$

or

$$F_{LQF} = (LQF) - 1.0 = 0 \qquad (16)$$

where,

SF = Safety Factor along a failure surface at time t
LQF = Liquefaction Potential at time t

Further, the *conditional limit state probabilities* $F_{SF;LQF}$ are the probabilities that at a given intensity of the input α_i (which is included in the power spectrum of the process and specifically in S_0) the factor of

safety against slope or liquefaction failure is less than unity or equivalently

$$F_{SF;LQF} < 0.0 \qquad (17)$$

with slope or liquefaction failure occurring when $F_{SF;LQF} < 0$.

The statistical simulation process proceeds as follows:

- Selects the range of the various intensity levels of the input which in turn evaluate the power spectrum of the process and consequently the time history and the Fourier coefficients of the input forcing function $g(t)$. The response of the system is evaluated via Equation (6).
- For the same intensity value but for M vectors of the phase angle ϕ_i (randomly selected) the process of the first step is repeated. For each synthetic history at the intensity level the temporal variation of the Safety Factor or the Liquefaction Potential is evaluated. Figure 2 is a sample of a generated input base motion, shear stress and safety factor variation. The criteria for failure during any such simulated event are (a) safety factors drop below 1.0 or (b) the potential to liquefaction is greater than 1.0. The potential to liquefaction is evaluated based on the resulting dynamic shear stresses at a particular location (Figure 2).
- The probability of failure at any given intensity α_i is computed in the form

$$P\left[F_{SF;LQF} < 0 \| PGA = \alpha\right] = \frac{M_{fail}}{M} \qquad (18)$$

where, M_{fail} are the number of simulated earthquakes at $PGA = \alpha$ that induced failure and M is the total number of simulations.
It should be noted that the larger the number of simulations M at each level the better the probabilistic assessment.

- Repeating the process for the selected intensity range $(\alpha_i \ldots\ldots \alpha_k)$ a fragility curve is developed reflecting the susceptibility of the system to either mode of failure.

POROSLAM Probabilistic Analysis. Stochastic Approach

Consider the case when the input forcing function (earthquake or load) belongs to a *weakly* stationary process $a(t)$ of duration T, zero mean and autocorrelation and power spectral density functions given by the relations,

$$E\left[a\left(t\right)\right] = 0$$

$$E\left[a\left(t+\tau\right)a\left(t\right)\right] = R_{aa}\left(\tau\right)$$

$$\Phi_a = \frac{1}{2\pi}\int_{-\infty}^{\infty} R_{aa}\left(\tau\right)e^{-i\omega\tau}d\tau \qquad (19)$$

$$R_{aa}\left(\tau\right) = \int_{-\infty}^{\infty}\Phi_a\left(\omega\right)e^{i\omega\tau}d\omega$$

The synthesized time history

$$g\left(t\right) = 2\sum_{i=1}^{N}\sqrt{\Phi_a\left(\omega_i\right)\Delta\omega}cos\left(\omega_i t + \phi_i\right)$$

can be assumed to represent $a(t)$ as $N \rightarrow \infty$ and has both the mean and the autocorrelation of the stochastic process $a(t)$.

With Complex Unit Response Function of the multi-degree of freedom system $H(\omega)$ available for either unit base excitation or unit harmonic load, the following powerful relation holds,

$$\Phi_{out}\left(\omega\right) = H\left(\omega\right)\Phi_{inp}\left(\omega\right)H^{*T}\left(\omega\right) \qquad (20)$$

where Φ_{inpt} *and* Φ_{out} are the Power Spectral Densities of the input and output respectively. Provided that the excitation is stationary, the response is also stationary and all the mathematical relations pertaining to a stochastic process, which satisfies that criterion, hold. These statistical properties of the response process are listed below

$$\sigma_Y^2 = \int_0^{\infty}\Phi_Y\left(\omega\right)d\omega$$

$$\lambda_Y^{(i)} = \int_0^\infty \omega^i \Phi_Y(\omega)\, d\omega, \quad i = 1, 2, .. \tag{21}$$

By utilizing the statistical properties of Equation (21) the probability density function of the response quantity (say shear stress at a location) can be evaluated. For temporal variations of the shear stress as viewed in a liquefaction assessment process, for example, a *Rayleigh* or *Gaussian* probability density function $p(\tau)$ can represent the peak (or equivalently stress cycle) distribution. Since the key to failure is the number of **induced** stress cycles by the input one need to, in compliance with the statistical model, estimate the probable number of cycles. For a lightly damped system (narrow-band) the *expected equivalent cycles per unit time* can be estimated from

$$N_{eqv} = \frac{\omega_{eqv}}{2\pi} \qquad \omega_{eqv} = \sqrt{\frac{\lambda_Y^{(2)}}{\sigma_Y^2}} \tag{22}$$

so the total number of cycles for the duration T of the event are equivalently

$$N = \frac{\omega_{eqv} T}{2\pi}$$

and the number of cycles at a shear stress level τ_i

$$N(\tau_i) = \frac{\omega_{eqv} T}{2\pi} p(\tau_i) \tag{23}$$

For a particular soil medium for which a relation between the number of stress cycles of a given intensity required to cause failure exists, such as stress ratio vs. cycles in Figure 3, the failure potential can be viewed through the relation

$$Damage = \int_0^\infty \frac{N(\tau)}{N_{req}(\tau)} d\tau \tag{24}$$

where $N_{req}(\tau_i)$ is the number of stress cycles that can lead to failure at the stress level τ. The above expression is similar to the well known Miner's Linear Failure criteria and indicate failure when $Damage > 1.0$.

6. References

1. *POROSLAM. Two-Dimensional Dynamic Solution of Elastic Saturated Porous Media*, N. Simos, C.J. Costantino, C. Miller, Earthquake Research Center, City Univ. of New York.
2. *Seismic Risk Assessment of Small Earthdams*, C.J. Costantino, N. Simos, Y.T. Gu, Technical Report NCEER-91, Earthquake Research Center, City University of New York.
3. *Probabilistic Theory of Structural Dynamics*, Y.K. Lin, Krieger, 1976.
4. *Dynamics of Structures*, R.W. Clough, J. Penzien, McGraw Hill,1975.
5. *Liquefaction of Soils During Earthquakes*, Committee on Earthquake Engineering *et al*, National Academy Press, 1985.
6. *A simplified Procedure for Evaluating Soil Liquefaction Potential*, H.B. Seed, I.M. Idriss, Report No. EERC 70-9, 1970.
7. *Analysis of Soil Liquefaction: Niigata Earthquake*, H.B. Seed, I.M. Idriss, Journal of Soil Mechanics and Foundations Division, pp 83-108, 1967.
8. *Evaluation of Soil Liquefaction Potential for Level Ground During Earthquakes*, NUREG-0026, 1976.
9. *Representation of Irregular Stress Time Histories by Equivalent Uniform Stress Series in Liquefaction Analyses*, California University, PB-252 635, 1975.
10. *Cyclic Stress Conditions Causing Liquefaction of Sands*, K.L. Lee, H.B. Seed, Journal of Soil Mechanics and Found. Div., No. SM1, pp.47-70, 1967.
11. *Comparison of Dynamic Analyses for Saturated Sands*, W.D.L. Finn, G.R. Martin, M.K.W. Lee, Proc. of the ASCE Geotech. Div., Vol.1, pp. 472-491, 1978.
12. *Compilation of Cyclic Triaxial Liquefaction Test Data*, J.M. Ferrito, J.B. Forest, G. Wu, Geotechnical Testing Journal, Vol 2, No.2, pp. 106-113, 1979.

13. *The Generation and Dissipation of Pore Water Pressures During Soil Liquefaction*, California University, PB-252 648, 1975.

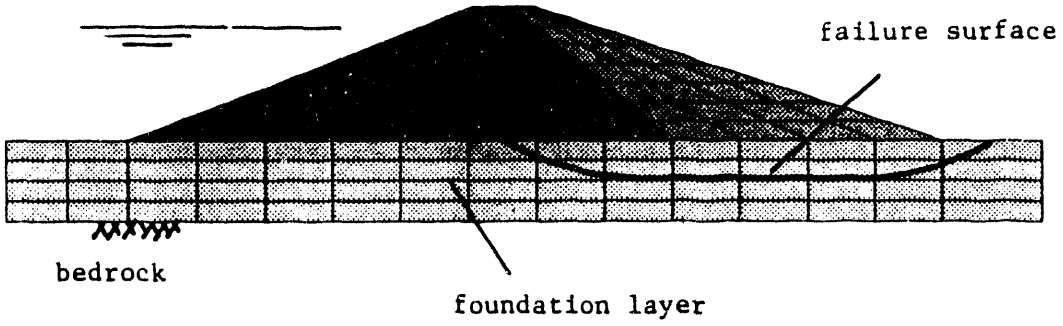

Figure 1. A typical earthen dam cross section

DISCLAIMER

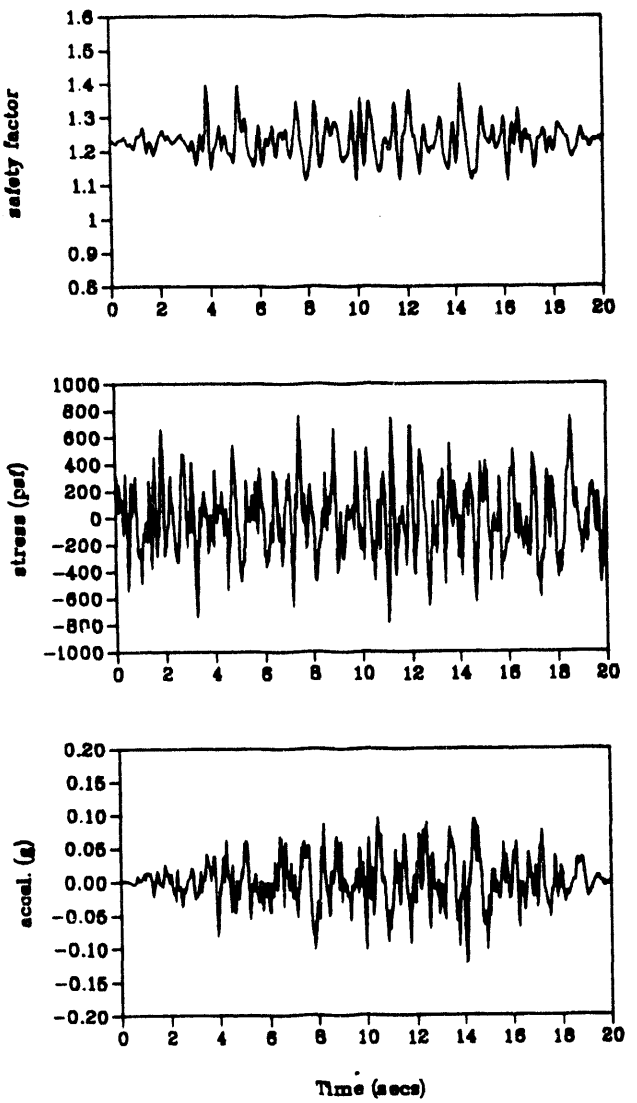

Figure 2. Base excitation, induced shear stress and temporal variation of factor of safety along a failure surface

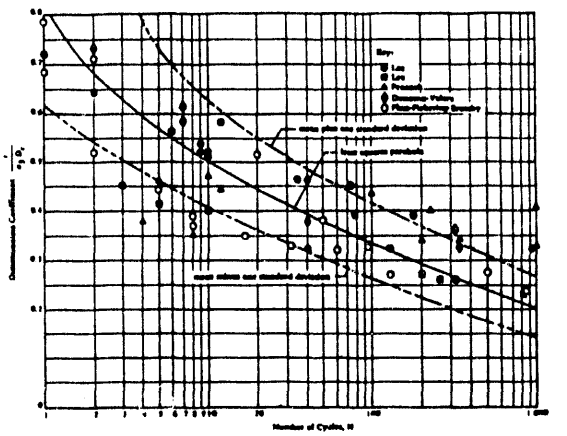

Figure 3. Typical strength data for sands

DATE
FILMED
9/26/94

END